Important Notice to Authors

Attached is a PDF proof of your forthcoming article in *Physical Review Letters*. The article accession code is LH15516.

Your paper will be in the following section of the journal: LETTERS — Condensed Matter: Structure, etc.

Please note that as part of the production process, APS converts all articles, regardless of their original source, into standardized XML that in turn is used to create the PDF and online versions of the article as well as to populate third-party systems such as Portico, CrossRef, and Web of Science. We share our authors' high expectations for the fidelity of the conversion into XML and for the accuracy and appearance of the final, formatted PDF. This process works exceptionally well for the vast majority of articles; however, please check carefully all key elements of your PDF proof, particularly any equations or tables.

Figures submitted electronically as separate PostScript files containing color appear in color in the online journal. However, all figures will appear as grayscale images in the print journal unless the color figure charges have been paid in advance, in accordance with our policy for color in print (http://journals.aps.org/authors/color-figures-print).

No further publication processing will occur until we receive your response to this proof.

Specific Questions and Comments to Address for This Paper

The numbered items below correspond to numbers in the margin of the proof pages pinpointing the source of the question and/or comment. The numbers will be removed from the margins prior to publication.

1. Please note that APS does not allow usage of mixed casing in the acronym. Could you please confirm the change of "cASW" to "CASW" throughout.
2. Please note that as per PRL journal style the term "endpoint" has been changed to "end point" throughout Letter. Please check.
3. Please note that only named scholarships can be listed in the acknowledgments.
4. Please review the funding information section of the proof's cover letter and respond as appropriate. We must receive confirmation that the funding agencies have been properly identified before the article can publish.
5. NOTE: External links, which appear as blue text in the reference section, are created for any reference where a Digital Object Identifier (DOI) can be found. Please confirm that the links created in this PDF proof, which can be checked by clicking on the blue text, direct the reader to the correct references online. If there is an error, correct the information in the reference or supply the correct DOI for the reference. If no correction can be made or the correct DOI cannot be supplied, the link will be removed.
6. It is PRL style to include all the author names in journal references for 10 or few authors. Please verify all author names in expanded lists in Ref. [35].

Titles in References

The editors now encourage insertion of article titles in references to journal articles and e-prints. This format is optional, but if chosen, authors should provide titles for *all* eligible references. If article titles remain missing from eligible references, the production team will remove the existing titles at final proof stage.

Funding Information

Information about an article's funding sources is now submitted to CrossRef to help you comply with current or future funding agency mandates. Please ensure that your acknowledgments include all sources of funding for your article following any requirements of your funding sources. CrossRef's FundRef registry (http://www.crossref.org/fundref/) is the definitive registry of funding agencies. Please carefully check the following funder information we have already extracted from your article and ensure its accuracy and completeness:

- Science and Technology Facilities Council, FundRef ID http://dx.doi.org/10.13039/501100000271 (United Kingdom of Great Britain and Northern Ireland)
- European Social Fund, FundRef ID http://dx.doi.org/10.13039/501100004895 (Kingdom of Belgium)
- European Research Council, FundRef ID http://dx.doi.org/10.13039/501100000781 (Kingdom of Belgium)
- Austrian Science Fund, FundRef ID http://dx.doi.org/10.13039/501100002428 (Republic of Austria)
- Seventh Framework Programme, FundRef ID http://dx.doi.org/10.13039/501100004963 (Kingdom of Belgium)

Other Items to Check

- Please note that the original manuscript has been converted to XML prior to the creation of the PDF proof, as described above. Please carefully check all key elements of the paper, particularly the equations and tabular data.
- Title: Please check; be mindful that the title may have been changed during the peer review process.
- Author list: Please make sure all authors are presented, in the appropriate order, and that all names are spelled correctly.
- Please make sure you have inserted a byline footnote containing the email address for the corresponding author, if desired. Please note that this is not inserted automatically by this journal.
- Affiliations: Please check to be sure the institution names are spelled correctly and attributed to the appropriate author(s).
- Receipt date: Please confirm accuracy.
- Acknowledgments: Please be sure to appropriately acknowledge all funding sources.
- References: Please check to ensure that titles are given as appropriate.
- Hyphenation: Please note hyphens may have been inserted in word pairs that function as adjectives when they occur before a noun, as in "x-ray diffraction," "4-mm-long gas cell," and "*R*-matrix theory." However, hyphens are deleted from word pairs when they are not used as adjectives before nouns, as in "emission by x rays," "was 4 mm in length," and "the *R* matrix is tested."
  Note also that Physical Review follows U.S. English guidelines in that hyphens are not used after prefixes or before suffixes: superresolution, quasiequilibrium, nanoprecipitates, resonancelike, clockwise.
- Please check that your figures are accurate and sized properly. Make sure all labeling is sufficiently legible. Figure quality in this proof is representative of the quality to be used in the online journal. To achieve manageable file size for online delivery, some compression and downsampling of figures may have occurred. Fine details may have become somewhat fuzzy, especially in color figures. The print journal uses files of higher resolution and therefore details may be sharper in print. Figures to be published in color online will appear in color on these proofs if viewed on a color monitor or printed on a color printer.
- Overall, please proofread the entire *formatted* article very carefully. The redlined PDF should be used as a guide to see changes that were made during copyediting. However, note that some changes to math and/or layout may not be indicated.

Ways to Respond

- ***Web:*** If you accessed this proof online, follow the instructions on the web page to submit corrections.
- ***Email:*** Send corrections to aps-robot@luminad.com. Include the accession code LH15516 in the subject line.
- ***Fax:*** Return this proof with corrections to +1.855.808.3897.

If You Need to Call Us

You may leave a voicemail message at +1.855.808.3897. Please reference the accession code and the first author of your article in your voicemail message. We will respond to you via email.

Neutron Scattering Analysis of Water's Glass Transition and Micropore Collapse in Amorphous Solid Water

Catherine R. Hill,[1] Christian Mitterdorfer,[2] Tristan G. A. Youngs,[3] Daniel T. Bowron,[3] Helen J. Fraser,[2] and Thomas Loerting[2,*]

[1]*Department of Physical Sciences, The Open University, Walton Hall, Milton Keynes MK7 6AA, United Kingdom*
[2]*Institute of Physical Chemistry, University of Innsbruck, Innrain 80/82, A-6020 Innsbruck, Austria*
[3]*ISIS Facility, Rutherford Appleton Laboratory, Harwell Oxford, Didcot, Oxon OX11 0QX, United Kingdom*

(Received 28 August 2015)

The question of the nature of water's glass transition has continued to be disputed over many years. Here we use slow heating scans (0.4 K min^{-1}) of compact amorphous solid water deposited at 77 K and an analysis of the accompanying changes in the small-angle neutron scattering signal, to study mesoscale changes in the ice network topology. From the data we infer the onset of rotational diffusion at 115 K, a sudden switchover from nondiffusive motion and enthalpy relaxation of the network at <121 K to diffusive motion across sample grains and sudden pore collapse at >121 K, in excellent agreement with the glass transition onset deduced from heat capacity and dielectric measurements. This indicates that water's glass transition is linked with long-range transport of water molecules on the time scale of minutes and, thus, clarifies its nature. Furthermore, the slow heating rates combined with the high crystallization resistance of the amorphous sample allow us to identify the glass transition end point at 136 K, which is well separated from the crystallization onset at 144 K—by contrast to all earlier experiments in the field.

DOI:

Water's glass transition has remained controversial for decades [1]. A key question is whether or not the endothermic feature observed in calorimetry experiments upon heating amorphous ices indicates transition from the glassy state to the deeply supercooled liquid. McMillan and Los were the first to detect the subtle increase in water's heat capacity near 137 K, which they assigned to the glass transition of water [2]. Historically, other researchers were unable to observe the same effect, either because it is so weak, or because it is obscured by enthalpy relaxation effects when unannealed samples are used [3]. In order to disentangle the exotherm caused by enthalpy relaxation from the increase in heat capacity caused by the glass transition, well-annealed amorphous ice samples have to be used. Typically, such samples are kept for 90 min at 129 K and then cooled back to 77 K prior to the calorimetry scan [4–6]. A glass-transition onset temperature $T_{g,\mathrm{onset}}$ of 136 ± 2 K was detected at standard heating rates of 30 K min^{-1} for a range of well-annealed amorphous ices, including (a) LDA (low-density amorphous ice) [6], (b) HGW (hyperquenched glassy water) [4], and (c) cASW (compact amorphous solid water) [5]. The glass transition in high-density amorphous ice (HDA), has an onset temperature $T_{g,\mathrm{onset}}$ of 116 ± 2 K at ambient pressure, and has hence been called water's second glass transition [7].

In this work we deal exclusively with the nature of water's first, "traditional" glass transition. In LDA, cASW, and HGW ice "phases," the increase in heat capacity at the glass transition, Δc_p gauged from endothermic changes in calorimetry scans, amounts to about 1 J K^{-1} mol^{-1}, corresponding to one of the feeblest glass transitions ever detected. In addition, the whole width of the glass transition cannot be studied, because the exothermic phase change to crystalline ice terminates the glass transition before its end point can be observed [4–6,8,9].

For all these reasons, there has been significant speculation about the nature of the glass transition. The explanations fall into 5 broad areas: (i) a transition from the glassy to the liquid state involving diffusion [4–6], isotope exchange [10], and viscosity decrease [11], (ii) a transition from one glassy to another glassy state (of the ice), involving unlocking of re-orientational (torsional), but not translational diffusion and no change in viscosity [12], (iii) a pretransition, called the shadow glass transition [13,14], (iv) amorphous ice is crystal-like [15–17], or (v) it is an impurity effect [18].

Suggestions (i) and (iii) were tested by studying the heating and cooling rate dependence of water's glass transition [19]. The results were shown to be incompatible with scenario (iii) [19] and, consequently, suggestion (iii) was retracted [20]. Furthermore, these studies allowed us to show that ultraviscous water represents one of the strongest liquids known in terms of the Angell classification [20],

consistent with Ref. [21]. Recently, the fragility index of water near 136 K was demonstrated to have the lowest value known for any liquid [7,22]; i.e., water is "super-strong" near T_g [23].

The open question that remains to be addressed is whether diffusive, translational motion is involved in water's glass transition. We have used small angle neutron scattering to study cASW, which is slowly heated at $\sim$0.4 K min^{-1}, and focus our attention on the structural changes associated with the collapse of the network of micropores in the ice as it warms. The advantage of this experimental technique over calorimetry experiments done in the past is that the competing endothermic and exothermic changes in the ice are not superimposed, so it allows unprecedented insight into the molecular processes occurring in the vicinity of T_g.

About 1 g of D_2O-cASW was produced by slow water vapor deposition onto a copper plate held at 77 K. Dosing occurred in the line of sight mode (nonbaffled supersonic flow) as described in our earlier work [24]. The sample was characterized after recovery from the vacuum chamber, showing it was free of contamination with crystalline ice using x-ray diffraction and thermal analysis [24]. Nitrogen adsorption BET isotherms at 77 K show the pores to be micropores, i.e., of diameter $d \leq 21$ Å and total volume $\approx$0.17–0.21 cm^3 g^{-1} [25]. Compared with the volume of pore-free ASW of 1.08 cm^3 g^{-1} the total volume fraction of pores thus amounts to about $1/6 - 1/5$. The recovered samples were then stored under liquid N_2, shipped (with cryogenic containment) to the NIMROD instrument at ISIS, and transferred into a null-scattering TiZr alloy cell, all under liquid N_2, as described in Ref. [24]. The sample was then heated at $\approx$0.4 K min^{-1} from 77 to 144 K, with four isothermal "pauses": of 20 min at 93 K, 35 min at 117 K, 55 min at 136 K, and 68 min at 144 K. According to calorimetric studies $T_{g,\mathrm{onset}}$ is directly dependent on the heating rate, appearing at 124 K for heating rates of 0.17 K min^{-1} [8], 136 K for heating rates of 30 K min^{-1} [4–6], and 176 K for heating rates of 6×10^6 K min^{-1} [9]. Based on the rates used in our experiments, $T_{g,\mathrm{onset}} \approx 124$ K.

Small angle neutron scattering is a nondestructive method particularly suitable for the study of granular or porous structures with dimensions between 10 and 1000 Å [26]. The power of the near- and intermediate range order diffractometer (NIMROD) is that it allows simultaneous observation of the mesoscale and intra- and intermolecular bonding. The broad peaks centered at 1.7 Å^{-1} in Figs. 1(a)-1(c) are indicative of cASW. Below 144 K, no signs of crystallinity were detected at $Q > 1$ Å^{-1}, indicating that regardless of any other changes in the ice structure, the intermolecular bonding remains amorphous throughout. Crystallization was clearly detected a few minutes into the isothermal pause at 144 K [see narrowing at 1.7 Å^{-1} and appearance of Bragg peaks in Fig. 1(d)]. The slope and the shape of the small angle neutron signal at $Q < 1$ Å^{-1}

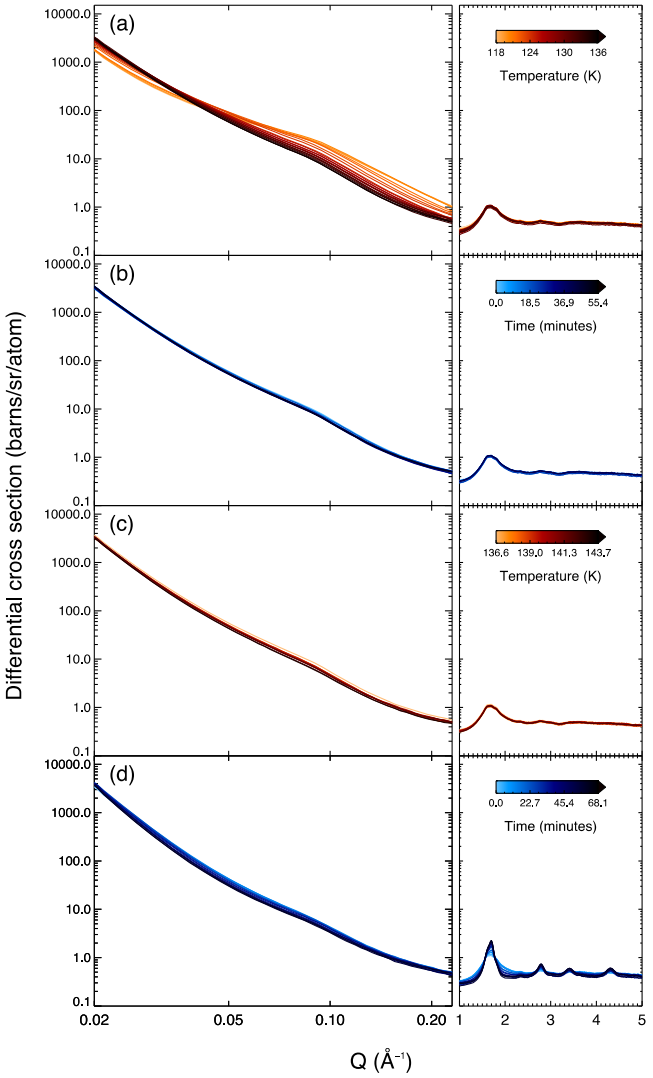

FIG. 1. Raw NIMROD neutron scattering data covering both the mesoscale and molecular scale scattering cross sections simultaneously. The evolution of the spectra is shown as a function of (a), (c) temperature, heating at 0.4 K min^{-1} and (b),(d) time, during an isothermal pause. The time-temperature evolution (in approximately 1 K steps or 5 min intervals) is indicated by the decreasing color scale of each plot.

can be used to investigate the properties of the ice on the mesoscale. It is evident from Figs. 1(a)–1(c) that the neutron scattering cross section is nonzero. Features common to our earlier work (and described in detail therein) [24] indicate our cASW sample is both granular (the "slope") and porous (the "hump").

The raw data were analyzed using several approaches: First, we used a model-free approach to extract specific surface area (SSA) from the scattered intensity at small angles (see Ref. [24]). Standard linear plots $I(Q) \times Q^d$ (with d equal 2.5 or 3.0) versus Q show a "pseudopeak" at the distances corresponding to periodic pore spacings of $\approx$70 Å [24]. These pseudopeaks can be seen clearly up to

120 K, but then progressively disappear between 120 and 135 K. Direct power-law fitting is used to extract the Porod exponent β associated with the mass fractal dimension of the material. Second, we tried to fit the data using models. Whereas the Maxwell model assuming spherical pores fails, the Guinier-Porod (GP) model fits the data well [24]. The fit parameters are attributed to the pore shape (s parameter), pore-size (radius of gyration R_G), and nature of the interface between granules (d_{GP} parameter). The outcomes of these analyses are shown in detail in Fig. 2. The parameters defining the ice structure can be broadly divided into three regimes—the temperature range prior to around 115 K where practically no changes occur, 115–144 K (the focus of the remainder of this Letter), and crystallization at 144 K and beyond.

The shape of the pores is never spherical, but much closer to cylindrical at 77–120 K, ($s \approx 1.5$ [Fig. 2(d)]. Beyond 121 K the pores progressively change shape: first they shrink along one axis and develop to 2D lamellae ($s = 2$) and then they disappear by 136 K (s approaches 3). Even from visual inspection a drastic height loss of the ice sample can be noticed: the ice sample changes from rugged, with protrusions of about 1 cm in length, to smooth, with an overall thickness of a couple of mm. Similar changes were monitored by optical interference measurements [27]. Not only the pore shape, but also β [Fig. 2(b)] and R_G [Fig. 2(e)] remain approximately constant at 77–120 K, even during the two "isothermal pause" periods at 93 and at 117 K. In other words, the network of water molecules is translationally immobile both during heating and isothermal annealing on a time scale of hours at <120 K.

The SSA does not decrease at 80–120 K, but remains either constant or increases slightly with temperature. Both of the latter scenarios are consistent with the uncertainties related to the $\mathrm{I}(Q) \times Q^4$ analysis. One way to account for a SSA increase would be if pore clustering occurs in the ice, leading to larger (internal) pore surface areas in addition to the ice interface to the vacuum. Such a pore clustering was inferred by positron-annihilation spectroscopy [28] and recent kinetic Monte Carlo ice simulations [29]. Our cASW ice sample, however, exhibits no pore clustering—the pore shape, the radius (R_G), and periodic spacings between pores all remain constant. Likewise, neither d_{GP} or β are changing at 80–120 K. Thus, the SSA either remains constant at 80–120 K or increases slightly due to the overall expansion of the bulk icy material. The main difference to other experiments [27,30–32] showing a continual decrease in SSA with temperature is their deposition mode for ASW samples, which is more akin to the "baffled" flow conditions used in our earlier work. Using baffled deposition we also saw the decrease of SSA with temperature [24]. The major difference between "nonbaffled, supersonic" flow conditions used here and baffled flow was explained in Ref. [33].

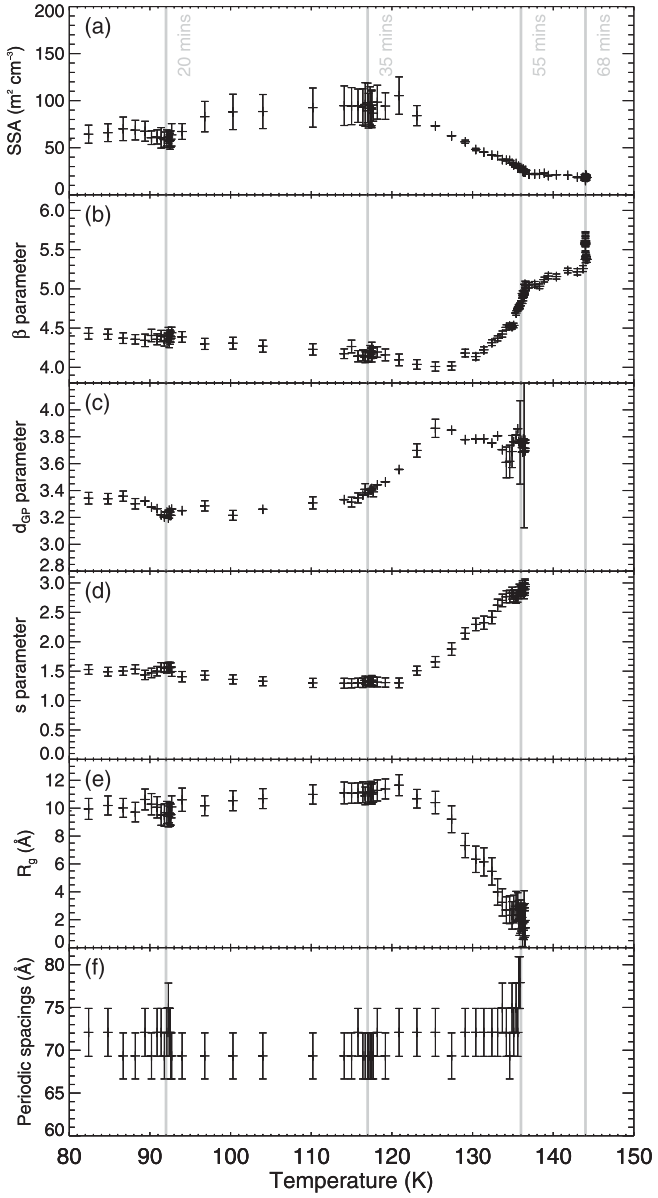

FIG. 2. Evolution of the key structural parameters derived from the neutron scattering differential cross section data with temperature. Isothermal stopping points are indicated by gray lines at 92, 117, 136, and 144 K, with the isothermal pause given alongside each line in minutes. (a) Specific surface area calculated from the plateau in $\mathrm{I}(Q) \times Q^4$ vs Q. (b) Porod β parameter, determined from the low Q region at $Q =$ 0.02–0.03 Å^{-1} where $\mathrm{I}(Q) = D \times Q^{\beta}$, indicating the size, shape, and surface roughness of the granular scattering material. (c) Guinier-Porod d parameter, calculated from the Guinier Porod fits to the data between around $Q = 0.045$–0.2 Å^{-1}, describing the internal surface roughness of the pores, where $d = 3$ indicates a rough surface and $d = 4$ indicates that the surface is smooth, on this length scale. (d) GP s parameter, representing the geometry of the pores, where $s = 0 =$ sphere, $s = 1 =$ cylinder, $s = 2 =$ platelets $\rightarrow 3$ as the pore collapses and disappears. (e) GP radius of gyration R_g and (f) periodic spacing between pores, as calculated from in $\mathrm{I}(Q) \times Q^d$ vs Q (where $d = 2.5$ or 3).

On the mesoscale our samples drastically change above 121 K, and such changes occur prior to, and independently of, the amorphous to crystalline phase change. In all data, Figs. 2(a)–2(e), it is clear that significant changes are occurring during heating, particularly in the 121–136 K range: SSA and R_G suddenly start to drop appreciably, and s rises steeply. This indicates a new type of molecular motion governing the evolution of the mesoscale topology. This motion involves the collapse of the cylinderlike pores of $R_G \approx 11$ Å [Fig. 2(e)] and $d \leq 21$ Å [25]. Large-scale transport of water molecules over at least 10 Å (pore radius) is necessary to achieve these kinds of changes. Assuming water self-diffusion and a random walk, the minimal self-diffusion coefficient D required to achieve these mesoscale changes can be estimated: $D > 10^{-18}$ cm^2 s^{-1} is required using a mean-square displacement $\langle x^2 \rangle \approx 100$ Å^2 and $t \approx 2500$ sec as the time it takes to complete the pore collapse between 120 and 136 K. Consistent with this, Ghesquiére *et al.* calculate $D \approx 10^{-12}$ cm^2 s^{-1} in this temperature range for a cASW sample based on MD trajectories on the μs time scale, whereas D is too small to be determined at lower temperatures [34]. We, therefore, attribute the observed structural changes to be a result of diffusive, translation motion. That is, from these data we infer the onset of molecular mobility (translational diffusion) and pore collapse occurs in our cASW sample at 121 ± 1 K. This is very close to the calorimetric $T_{g,\mathrm{onset}}$ of 124 K [8]. At about the same temperature surface diffusion of a range of adsorbates [35] and isotopic mixing is initiated [10].

The Porod exponent β, and Guinier-Porod exponent d_{GP} indicate a third regime of change within the ice structure. From the start of the heating cycle β continually decreases very slightly, reaching a minimum value at around 126 K before reversing direction and increasing again. β is not related to the diffusive motion associated with pore collapse, nor changes in the SSA, but represents the nature of the interface between individual granules, as well as their shapes [24]. This parameter continues to change even in the isothermal waiting period at 144 K, reflecting the sintering of ice granules as crystallization occurs. d_{GP} starts increasing at around 115 K, which we interpret to reflect the onset of rotational (torsional) motion of the water molecules. Such motion leads to smoothing of the pore surfaces (reflected by an increase in d_{GP}), without pore collapse occurring (no changes in R_G or s). Pore collapse is accompanied by smoothing and shape changes in the ice grains (rapid increase in β), i.e., free molecular movement of H_2O. That is, cASW is in a liquid state above T_g. By 136 K the rapid changes in SSA and β cease, and in the subsequent heating stage from 136–144 K change relatively little, indicating the end of the glass transition. The process is complete long before the ASW to I_c transition at 144 K, 27 min into the isothermal step, which can be identified in both Figs. 1(d) and 2(b) (discontinuous jump in the β parameter from 5.41 to 5.57). That is, there is a separation between the glass transition end point $T_{g,\mathrm{end}}$ and the crystallization onset T_X. Such a separation was not found in earlier work on LDA-type samples. This is because in previous studies heating rates faster by about 2 orders of magnitude were employed [4–6]. In case of the calorimetry study by Handa *et al.* [8] the heating rate is comparable, but they were using an LDA-I sample that started to crystallize at 133 ± 1 K, i.e., which is much less crystallization resistant than the cASW sample studied by us [6]. The width of the glass transition is thus 15 K. For comparison, in earlier calorimetry work, a width of about 12 K was found between $T_{g,\mathrm{onset}}$ and T_X [4–6]. In other words, $T_{g,\mathrm{end}}$ would appear just slightly above the crystallization onset in the calorimetry scans at 10–30 K min^{-1}.

Thus, our data enable us to come back to the original purpose of our work—to describe the nature of water's glass transition, and distinguish between the five different hypotheses presented in the literature to explain the phenomenon. If just rotational (torsional) motion of water molecules at fixed oxygen positions, and/or point defect mobility similar to that known in crystalline ice was occurring near $T_{g,\mathrm{onset}}$, as suggested in (ii) [12], then the pore collapse would not occur. Clearly this regime exists in the ice, between 115 and 121 K, leading to pore surface smoothing, but not accompanied by a glass transition (or pore collapse), ruling out hypothesis (ii). The high Q neutron scattering cross section data indicate an amorphous nature of the ice throughout the glass transition temperature range. The possibility of nanocrystalline ice [explanation (iv)] is ruled out by the low translational mobility typically seen in crystalline ice; i.e., pore collapse would not occur upon heating nanocrystalline ice. Previous work shows that ASW with "filled" micropores, covering a wide range of adsorbates and exposures, also experience pore collapse, like "pure" cASW [36]. Thus, impurities as put forward in explanation (v) are not driving the pore collapse. Instead it is driven from the reorientation of the hydrogen-bond network of water molecules itself [34]. The explanation of water's glass transition consistent with all the observations is (i) long-range diffusion brings cASW into an ultraviscous state, leading to mass-transport of water molecules in the sample. The increase in heat capacity seen in calorimetry experiments [8] and the time scale of about 100 sec seen in dielectric relaxation spectra near 124 K [7] is, thus, associated with long-range translational diffusion of water molecules.

In conclusion, we have analyzed small-angle neutron scattering data in amorphous solid water. This analysis shows very subtle changes attributable to pore surface smoothing and cooperative, nontranslational motion of water molecules of water molecules set in at 115 K. Starting at 121 K the changes are much faster and reach completion at about 136 K, i.e., within about 40 min at heating rates of ≈ 0.4 K min^{-1}. This indicates that onset of

rotational motion precedes onset of translational motion, and that $T_{g,\mathrm{end}}$ is reached at 136 K. This is notable because crystallization is only detected at 144 K. Thus, by contrast to earlier investigation on water's glass transition [4–6,8,9], there is a good separation between $T_{g,\mathrm{end}}$ and T_X, which allows us to determine the glass transition width to be 15 K. These changes are associated with water molecules mobile enough to reach mean-square displacements $\langle x^2 \rangle$ exceeding 100 $\mathrm{Å}^2$, i.e., long-range, diffusive motion necessary to cause the collapse of the micropores and the $3D \rightarrow 2D$ topology change. The time scale extracted from the present work agrees with the time scale from calorimetry [4–6,8,9] and dielectric experiments [7] on well-annealed samples (after the network collapse). That is, the motion of water molecules at >121 K in annealed, compact ASW samples takes place at the same time scale as the motion of water molecules causing the transition from porous ASW to compact ASW. Again, this is only possible if one assumes this motion is translational and diffusive in character. Furthermore, the effect is not a surface effect, but rather a bulk effect. The effect is also inconsistent with the idea of a crystal-like nature. The nature of water's glass transition, therefore, is glass to liquid, but not glass to glass or crystal-like to crystal-like. Our work also provides the relevant time scales to be investigated using methods probing dynamics directly rather than inferring the dynamics based on the mesoscopic structural changes as done here. The time scales of relevance can, for instance, be probed using broadband dielectric relaxation spectroscopy, spin echo ^{2}H NMR, or quasielastic neutron scattering, which will be the focus of future work.

Experiments at the ISIS Pulsed Neutron and Muon Source were supported by a beam time allocation from the Science and Technology Facilities Council. We gratefully acknowledge the ESF Short visit grant (MicroDICE) for C. M. The study is financed by a grant from the European Research Council (ERC Starting Grant SULIWA) and the Austrian Science Fund FWF (bilateral French-Austrian project I1392). C. R. H. acknowledges support from The Open University. H. J. F. acknowledges the EU LASSIE FP7 ITN initiative (Laboratory Astrochemical Surface Science in Europe) Grant Agreement No. 238258 for her participation in this work.

*thomas.loerting@uibk.ac.at

[1] S. Capaccioli and K. L. Ngai, J. Chem. Phys. **135**, 104504 (2011).
[2] J. A. McMillan and S. C. Los, Nature (London) **206**, 806 (1965).
[3] C. A. Angell, W. J. Sichina, and M. Oguni, J. Phys. Chem. **86**, 998 (1982).
[4] G. P. Johari, A. Hallbrucker, and E. Mayer, Nature (London) **330**, 552 (1987).
[5] A. Hallbrucker, E. Mayer, and G. P. Johari, Philos. Mag. B **60**, 179 (1989).
[6] M. S. Elsaesser, K. Winkel, E. Mayer, and T. Loerting, Phys. Chem. Chem. Phys. **12**, 708 (2010).
[7] K. Amann-Winkel, C. Gainaru, P. H. Handle, M. Seidl, H. Nelson, R. Bohmer, and T. Loerting, Proc. Natl. Acad. Sci. U. S. A. **110**, 17720 (2013).
[8] Y. P. Handa and D. D. Klug, J. Phys. Chem. **92**, 3323 (1988).
[9] A. Sepúlveda, E. Leon-Gutierrez, M. Gonzalez-Silveira, C. Rodríguez-Tinoco, M. T. Clavaguera-Mora, and J. Rodríguez-Viejo, J. Chem. Phys. **137**, 244506 (2012).
[10] R. S. Smith and B. D. Kay, Nature (London) **398**, 788 (1999).
[11] G. P. Johari, J. Phys. Chem. B **102**, 4711 (1998).
[12] M. Fisher and J. P. Devlin, J. Phys. Chem. **99**, 11584 (1995).
[13] Y. Yue and C. A. Angell, Nature (London) **427**, 717 (2004).
[14] N. Giovambattista, C. A. Angell, F. Sciortino, and H. E. Stanley, Phys. Rev. Lett. **93**, 047801 (2004).
[15] J. S. Tse, K. H. Tan, and J. M. Chen, Chem. Phys. Lett. **174**, 603 (1990).
[16] H. Schober, M. M. Koza, A. Tolle, C. Masciovecchio, F. Sette, and F. Fujara, Phys. Rev. Lett. **85**, 4100 (2000).
[17] V. P. Shpakov, P. M. Rodger, J. S. Tse, D. D. Klug, and V. R. Belosludov, Phys. Rev. Lett. **88**, 155502 (2002).
[18] V. Sadtchenko, C. F. Giese, and W. R. Gentry, J. Phys. Chem. B **104**, 9421 (2000).
[19] I. Kohl, L. Bachmann, E. Mayer, A. Hallbrucker, and T. Loerting, Nature (London) **435**, E1 (2005).
[20] C. A. Angell, J. Phys. Condens. Matter **19**, 205112 (2007).
[21] S. M. McClure, D. J. Safarik, T. M. Truskett, and C. B. Mullins, J. Phys. Chem. B **110**, 11033 (2006).
[22] V. N. Novikov and A. P. Sokolov, Phys. Rev. Lett. **110**, 065701 (2013).
[23] C. A. Angell, C. T. Moynihan, and M. Hemmati, J. Non-Cryst. Solids **274**, 319 (2000).
[24] C. Mitterdorfer, M. Bauer, T. G. A. Youngs, D. T. Bowron, C. R. Hill, H. J. Fraser, J. L. Finney, and T. Loerting, Phys. Chem. Chem. Phys. **16**, 16013 (2014).
[25] E. Mayer and R. Pletzer, Nature (London) **319**, 298 (1986).
[26] A. K. Patra, S. Ramanathan, D. Sen, and S. Mazumder, J. Alloys Compd. **397**, 300 (2005).
[27] J.-B. Bossa, K. Isokoski, M. S. Valois, and H. Linnartz, Astron. Astrophys. **545**, A82 (2012).
[28] Y. C. Wu, J. Jiang, S. J. Wang, A. Kallis, and P. G. Coleman, Phys. Rev. B **84**, 064123 (2011).
[29] S. Cazaux, J.-B. Bossa, H. Linnartz, and A. G. G. M. Tielens, Astron. Astrophys. **573**, A16 (2015).
[30] H. J. Fraser, M. P. Collings, J. W. Dever, and M. R. S. McCoustra, Mon. Not. R. Astron. Soc. **353**, 59 (2004).
[31] U. Raut, M. Famá, B. D. Teolis, and R. A. Baragiola, J. Chem. Phys. **127**, 204713 (2007).
[32] R. S. Smith, N. G. Petrik, G. A. Kimmel, and B. D. Kay, Acc. Chem. Res. **45**, 33 (2012).
[33] E. Mayer and R. Pletzer, J. Chem. Phys. **80**, 2939 (1984).
[34] P. Ghesquière, T. Mineva, D. Talbi, P. Theulé, J. A. Noble, and T. Chiavassa, Phys. Chem. Chem. Phys. **17**, 11455 (2015).
[35] F. Mispelaer, P. Theulé, H. Aouididi, J. Noble, F. Duvernay, G. Danger, P. Roubin, O. Morata, T. Hasegawa, and T. Chiavassa, Astron. Astrophys. **555**, A13 (2013).
[36] R. A. Baragiola, in *Water in Confining Geometries*, edited by V. Buch and J. P. Devlin (Springer-Verlag, Heidelberg, 2003).